Design and Characterization of Porous Core Polarization Maintaining Photonic Crystal Fiber (PCF) for THz Guidance

Asmar Aming, Muhammad Uthman, Ratchapak Chitaree, Waleed Mohammed and B. M. Azizur Rahman, *Fellow, IEEE and Fellow, OSA.*

***Abstract*— An improved design of Teflon photonic crystal fiber (PCF) with a porous air-core is presented for low-loss terahertz guidance. Optimization of total power confinement in the air-holes, together both in the cladding and core regions, is carried out for both quasi-TE and quasi-TM polarizations by using a full-vectorial finite element method (FEM). To achieve the polarization maintenance, modal birefringence is enhanced by destroying the circular symmetry with the introduction of unequal size air-holes in the first ring.**

***Index Terms*—Finite Element method (FEM), Photonic Crystal Fiber (PCF), Porous-core PCF, modal birefringence, polarization maintaining PCF, and terahertz (THz) waveguides.**

I. Introduction

THE TERAHERTZ (THz) band is defined as the frequency region between 0.1-10 THz. Recently, interest in the THz technology has significantly been expanded due to their many potential applications. THz wave can penetrate through fabrics and polymer, useful for security screening for explosives [1, 2] and drugs [1] and with many potential medical applications [2-6] and this wave is much safer than the higher frequency X-ray. This can also be used in dental diagnostics [7]. THz wave operates at a higher frequency range than the microwave, which makes them a better c1andidate for high-speed communications [8] as well as for sensing applications [9]. Due to the expansion of THz waves' applications, many techniques have been developed to generate such waves and also to detect such radiation [10-12]. However, all the THz systems reported so far are based on the free-space transmissions due to lack of suitable waveguide. It is well known that wider application of electronics, photonics or microwave technology only happened when they were miniaturized and used guided-wave systems. So, development of low-loss waveguides is essential for the wider adaptation of this THz technology.

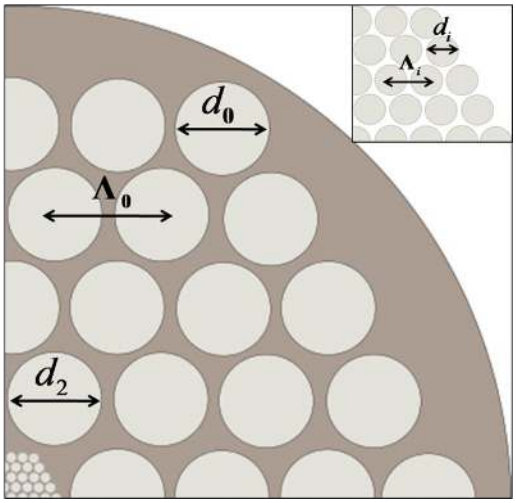

Fig.1. Cross-section of porous core PCF, $N_{core} = 4$ and $N_{clad} = 4$. Air holes are arranged in the cladding with Λ_0 = outer pitch, d_0 = outer diameter. Inset shows Λ_i = inner pitch, d_i = inner diameter in the porous core.

Previously, several conventional structures for guiding THz wave were demonstrated, such as bare metal wires [13], and circular and rectangular metal waveguides [14]. However, these structures suffered from very high losses. THz waves have negligible loss in dry-air, which has attracted the interest in developing low-loss waveguiding through the air. Pipe waveguide, which is a cylindrical metal tube, is an example of air-core waveguide with low-loss [15]. Subsequently, it has also been shown that a thin layer of dielectric coating inside the metal surface can reduce the modal loss significantly [16]. Dielectric structure has also been proposed for THz wave [17]. Typically, dielectric waveguide suffers of high modal loss due to the higher dielectric loss or conduction loss values of most commercially available materials in the THz region. Recently, new polymer materials have been developed to construct

Manuscript received …..

A. Aming. Author is with the Department of Physics, Faculty of Science, Mahidol University, Phayathai, Bangkok, Thailand 10400 and the City University London, School of Engineering and Mathematical Sciences, Northampton Square, London EC1V 0HB, U.K. (e-mail: a.asmar99@gmail.com)

M. Uthman. Author was with the City University London, School of Engineering and Mathematics Sciences, Northampton Square, London EC1V 0HB, U.K (e-mail: m.uthman@yahoo.com).

R. Chitaree. Author is with the Department of Physics, Faculty of Science, Mahidol University, Phayathai, Bangkok, Thailand 10400 (e-mail: rachapak.chi@mahidol.ac.th)

W. Mohammed. Author is Bangkok University, School of Engineering, Patum Thanee, Thailand 12120 (e-mail: waleed.m@bu.ac.th).

B.M. Azizur Rahman. Author is with City, University of London, School of Engineering and Mathematical Sciences, Northampton Square, London EC1V 0HB, U.K. (e-mail: B.M.A.Rahman@city.ac.uk).

flexible and low-loss dielectric waveguide such as polyethylene (PE) [18], low-density PE [19] , high-density PE [20, 21], polymethyl methacrylate (PMMA) [22, 23] and polycarbonate (PC). Among these, Topas [24] and Teflon [25, 26] are showing lower material loss and recently, several polymer waveguide structures have been reported based on these materials. On the other hand, hollow core [27] and microstructure fiber [28, 29] can also guide THz wave in air-core based on either antiresonant reflection (ARROW) or photonic bandgap. Porous core fiber [30-32] guides THz wave predominantly in air based on modified total internal reflection (TIR). These provide a very flexible waveguiding and relatively low absorption. Although guiding in air-clad with air-filled porous core offers low absorption loss, however, lower index contrast between core and cladding not only increases bending loss, but presence of any other material to support these guides will also perturb the guiding properties significantly. Atakaramians *et al.* [23] have *also* fabricated spider-web and rectangular porous THz polymer fiber with low-loss and low-dispersion and these can be practically used for THz biosensing.

A new-type of optical waveguide, microstructured optical fiber with air-holes running along its axis (commonly referred to as photonic crystal fiber, PCF) utilizes modified-TIR to guide the light inside a core is being widely used by the photonics community. Since air has a lower loss, having a large air fraction ratio makes it possible to reduce the loss for THz guiding, and PCF with porous clad has been reported by Han [21] and Goto [25]. Dielectric waveguide with porous core has also been reported [31]. Recently, a novel structure has been proposed by Uthman *et al*. [33] by combining both the advantages, using both porous core and porous clad. In this case, the structural geometry of the Teflon PCF were optimized to allow large fraction of the power to be confined in the porous core, which reduced the overall modal loss. Similarly, Hassani *et al.* [34] has reported that polymer PCF with porous core influences the modal properties significantly and increases the power confinement in the air-core and reduces the absorption losses.

A variety of PCF designs have been considered to exploit their single mode property, adjustable spot-size, dispersion and also higher modal birefringence properties. These are controllable by adjusting the geometrical parameters of a PCF. The design objective of Kejalakshmy *et al.* [35] was to increase the modal birefringence by breaking the natural symmetry of regular sized circular air-holes near the core in the first ring (d_2). A better performance was achieved if four out of six air-holes in the first ring is increased, $d_2 > d$ (Fig. 1.). Rahman *et al*. [36, 37] reported that in these cases, the quasi-TM mode (H_{11}^x) has a smaller effective index compared to the TE mode (H_{11}^y) and as the ratio between reduced air-holes diameter and pitch (d_2/Λ) increases this would yield a higher modal birefringence [38]. As d_2 is either decreased or increased, so that $d_2 \neq d$, and when their difference increases the modal index difference between the two fundamental polarized modes also increases.

In this paper, the design and optimization of a polarization maintaining porous core PCF is presented. A novel design approach is proposed where various waveguide parameters are optimized to reduce the modal loss and also to maintain the polarization state of THz wave by enhancing the modal birefringence of this waveguide.

II. NUMERICAL SOLUTION

The finite element method (FEM) has emerged as one of the most accurate, versatile and numerically efficient modal solution techniques. The FEM based on the full-vectorial **H**-field formulation is used in this study to obtain the modal solutions of porous core PCF. The intricate cross-section of a PCF can be represented by using many triangles of different shapes and sizes. This particular structure is very challenging to simulate, as the air-holes in core are three orders of magnitude smaller than the air-holes in cladding. The particular flexibility of using unequal size elements available in the FEM makes it as a preferable choice compared to the finite difference method, which not only uses inefficient regular spaced meshing, but also cannot represent well the curved dielectric interfaces of the circular air-holes. The modes in the high index contrast PCF with two-dimensional confinement are hybrid in nature, with all six components of the **E** and **H** fields being present and needs a full-vectorial approach. In this work, a **H**-field based rigorous full-vectorial FEM is used to obtain the modal solutions of PCF with air-holes arranged in triangular lattice in Teflon cladding operating at 1 THz. The **H**-field formulation developed earlier [39] is a valid approach for microwave and optical guided-wave devices including the intermediate terahertz range.

III. RESULTS

The structure designed here, the porous core along with the porous cladding, can be fabricated from low-loss Teflon operating in the THz frequency region. The number of air-holes rings in the cladding region is taken as, $N_{\text{clad}} = 4$, and number of air-hole rings inside the core, is also taken as, $N_{\text{core}} = 4$. However, they do not need to be equal. In this case, a similar size air-hole at the center of the core is also considered to further increase power fraction in the air-holes, which was not considered in our earlier work by Uthman *et al*. [33]. The structure consists of periodic air-holes with diameter *d*, and the pitch Λ, which is the distance between the two nearest holes. The well-developed conventional stack-and-draw technique can be used to fabricate the proposed PCF. With four rings inside the core, diameter of the core will be $9 \times \Lambda_i$, where Λ_i is the pitch of the inner air-holes or air-holes inside the core. It should be noted that, when the outer pitch denoted by Λ_0 is equal to the diameter of the porous core, in this case nine times $(2 * N_{\text{core}} + 1)$ of the inner pitch Λ_i, then such a porous core PCF would be easier to assemble by using the stack-and-draw technique with core and cladding canes of identical diameter. In this work, the refractive index of Teflon is taken as $1.445 + j0.000715$ which yields a bulk material loss of 0.3 cm^{-1} or 130 dB/m at the operating

frequency of 1 THz ($\lambda = 0.3$ mm) [34]. The available two-fold symmetry is exploited in the numerical simulations, where only a quarter of the cross section of the porous core PCF is considered, as shown in Fig.1. In the numerical simulations 500,000 first-order triangular elements of different sizes are used to represent a quarter of the structure.

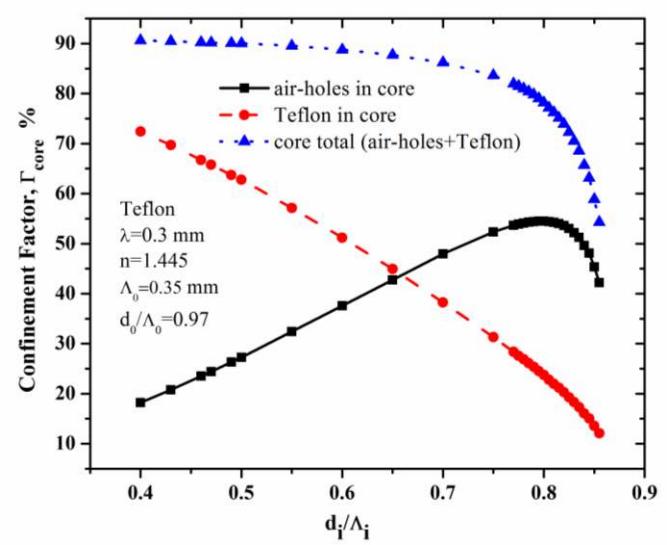

Fig.2. Variations of the power confinements for the fundamental quasi-TM (H_{11}^x) mode in porous core with the d_i/Λ_i

To support the total internal reflection (TIR) guidance along the waveguide core, the equivalent index of core should be greater than that of the clad, so that inner air-hole diameter/ inner pitch ratio (d_i/Λ_i) in the core needs to smaller than the outer air-hole diameter/pitch ratio (d_0/Λ_0) in the cladding. Variations of the power confinements, of the fundamental quasi-TM (H_{11}^x) mode in porous core with the d_i/Λ_i for a fixed d_0/Λ_0 are shown in Fig.2. Power confinements in the different regions of the core have been normalized to the total power. In this case, d_0/Λ_0 and Λ_0 are kept constants, at 0.97 and 0.35 mm, respectively and d_i/Λ_i is adjusted to achieve the maximum power confinement in the core air-holes. Generally, most PCF would support both the fundamental quasi-TE (H_{11}^y) and quasi-TM (H_{11}^x) modes. Each mode will reach to its cutoff condition when its effective index approaches the fundamental space filling mode (FSM) of the PCF cladding. Here, the effective index (n_e) is defined as $n_e = \beta/k_0$ where β is the propagation constant and k_0 is the wavenumber. It can be noted that as d_i/Λ_i increases, effective refractive index (n_{FSM}) of the core reduces. Since, d_0/Λ_0 is fixed, effective refractive index of cladding is fixed and thus the index contrast between core and cladding reduces as d_i/Λ_i increases. When d_i/Λ_i is large enough and approaches that of d_0/Λ_0, the PCF also approaches its modal cutoff, the total power confinement in core reduces, shown in Fig. 2 by the blue dotted line with triangles and the mode field extends to the cladding region. However, an increase in d_i/Λ_i also increases the air-fraction inside the core, and the share of the core-power guiding through air region also increases. As a result, the power confinement in the air-holes of the core increases initially with d_i/Λ_i and reaches its maximum value of 55%, as shown by a black solid line with squares, then reduces as the total core power confinement reduces when the mode approaches its cutoff condition.

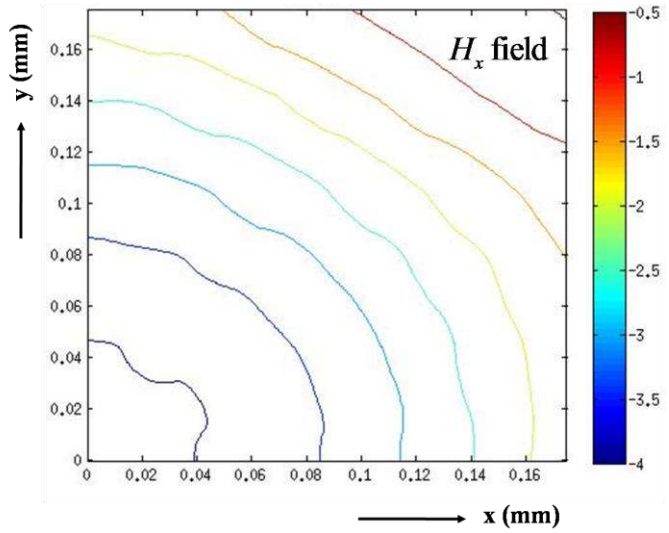

Fig.3. The H_x field of the fundamental quasi-TM (H_{11}^x) mode for $\Lambda_0 = 0.35$ mm, $d_0/\Lambda_0 = 0.97$ and $d_i/\Lambda_i = 0.6$

Figure 3 shows the H_x field profile of the fundamental quasi-TM (H_{11}^x) mode when $\Lambda_0 = 0.35$ mm, $d_0/\Lambda_0 = 0.97$ and $d_i/\Lambda_i = 0.6$. Due to available symmetry of the proposed structure, only a quarter of the field profile is shown here. The nature of the first contour close to the center $(x = 0, y = 0)$ clearly correlated with the presence of the air-holes in the first ring.

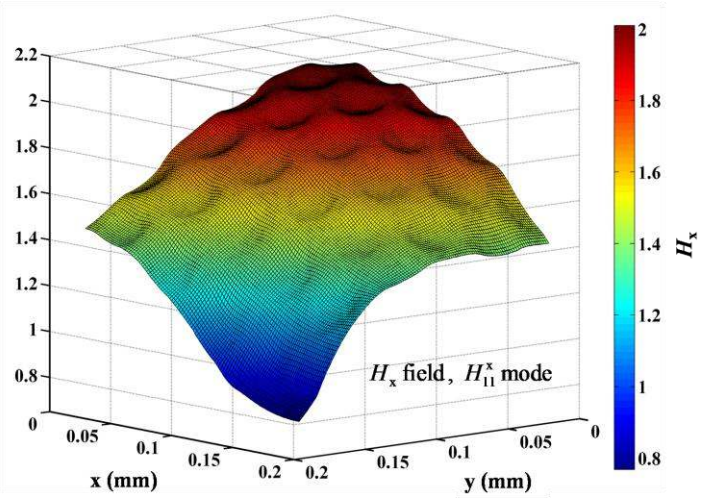

Fig.4. Locations of many tiny air holes in the core of PCF

As the core consists of very fine air-holes, so the dominant H_x field profile inside the core is also influenced by their presence, which is shown in Fig. 4. Here, locations of many tiny air holes in the core correspond to many small dips in the profile, like a golf ball surface. As the air-holes are far too small compared to the wavelength, reduction of the field values inside the low-index air-holes of the core is small.

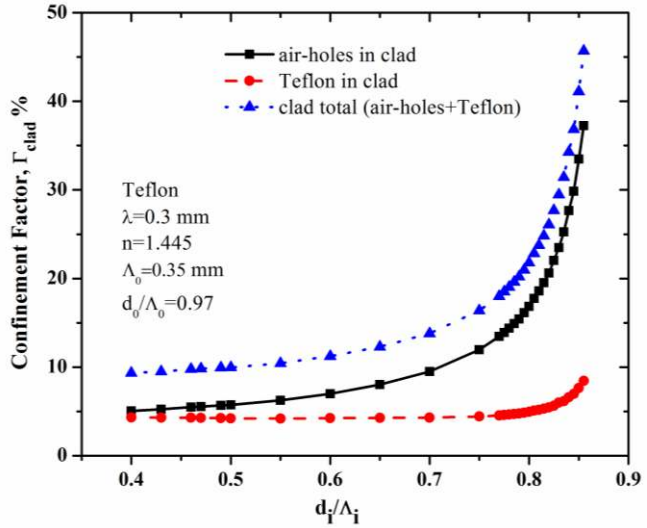

Fig.5. Variations of the power confinements of the fundamental quasi-TM (H_{11}^x) mode in cladding with the d_i/Λ_i

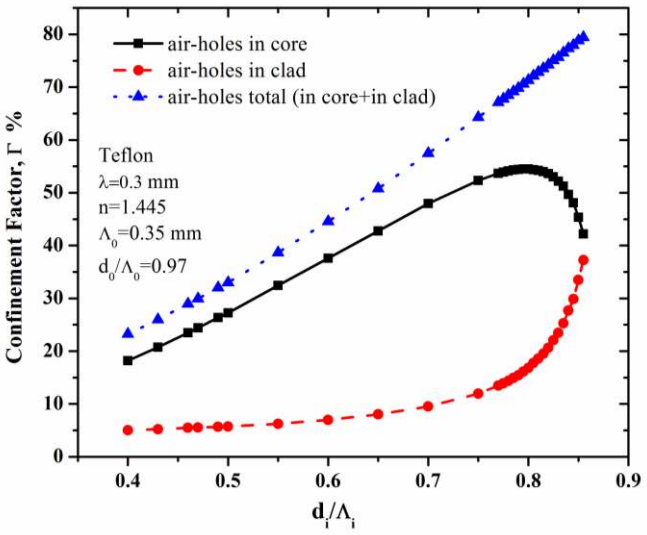

Fig.6. Variations of the power confinements of the fundamental quasi-TM (H_{11}^x) mode with the d_i/Λ_i

Variations of power fractions in the cladding are shown in Fig. 5. Earlier, in Fig.2, it was shown that as d_i/Λ_i increases, total power in the core reduces as the mode approaches its cutoff (when $d_i/\Lambda_i = 0.85$) and the power extends into the cladding region. Variation of the total cladding power with the d_i/Λ_i is shown by a blue dotted line with triangles in Fig.5. This confirms that the total power confinement in the cladding increases as d_i/Λ_i increases. However, as the d_i/Λ_i increases, so air-region in the cladding also increases, hence the share of the cladding power inside these air-holes also increases, which is shown by a black solid line with squares. As a result, as the total power in the cladding increases, the power fraction inside air-holes in the clad also increase but more rapidly, as shown in Fig. 5.

Figure 6 shows the total power confinement in the air-holes by combining the power confinement in all the air-holes, both in the cladding and also inside the core. A maximum power confinement of 80% can be observed with d_i/Λ_i as the mode approaches its cutoff. The total power confinement is limited by the power transfer from air-core (air-holes in core) to air-cladding (air-holes in the cladding) region when the cutoff condition is reached. This is indicated by the convergence of the power confinement fraction from the two regions.

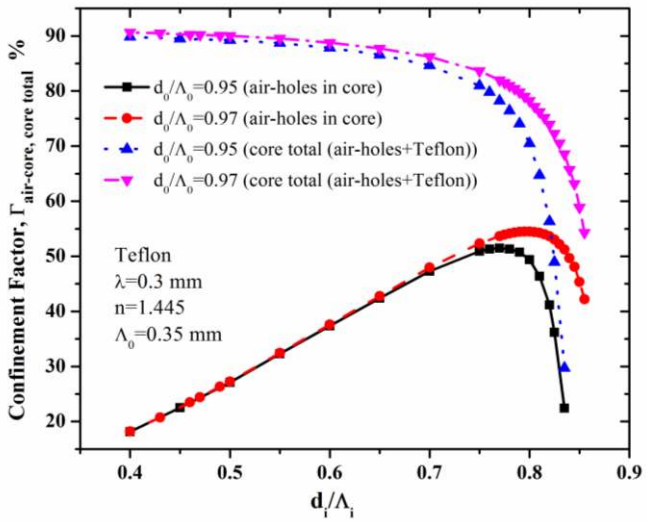

Fig.7. Variations of the power confinements of the fundamental quasi-TM (H_{11}^x) mode with the pitch $\Lambda_0 = 0.35$ mm.

Total power confinement in the air-holes depends on the intricate relation between the Λ, d_i/Λ_i and d_0/Λ_0 for a given operating frequency. Next, effect of the outer air-hole to pitch ratio (d_0/Λ_0) on the total power confinement is studied. Today, PCFs are routinely fabricated with pitch, Λ between 2 to 5 μm and d/Λ between 0.5 to 0.8 and operating at 1550 nm wavelength. This gives the required smallest silica strut-thickness about 400 nm. On the other hand, in design for THz guidance, when Λ_0 is as large as 350 μm, the required strut-thickness is thicker than 10 μm even when $d_0/\Lambda_0 = 0.97$ is considered, and this would be easy to fabricate. Although, it may be possible to fabricate a PCF with $\Lambda_0 = 350\,\mu$m and d_0/Λ_0 larger than 0.97, but here this work, the maximum value is taken as 0.97. Since, we are restricting the maximum value of d_0/Λ_0 to 0.97, so to study its effect a slightly smaller value of $d_0/\Lambda_0 = 0.95$ is taken for the comparison. Next, power confinement inside the air-core for different d_0/Λ_0 when the outer pitch $\Lambda_0 = 0.35$ mm is studied. A larger outer air-hole to pitch ratio $d_0/\Lambda_0 = 0.97$, demonstrates a reasonably well-confined mode inside the core. It can be

clearly observed from Fig. 7 that the maximum value of $\Gamma_{\text{air-core}} = 55\%$ at $d_i/\Lambda_i = 0.8$, with $d_0/\Lambda_0 = 0.97$, whereas a slightly smaller maximum value of 52% can be achieved at $d_i/\Lambda_i = 0.77$ when the d_0/Λ_0 is reduced to 0.95.

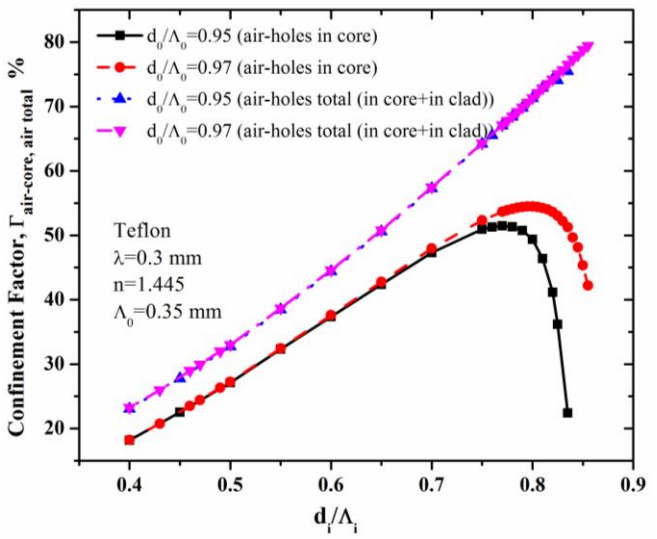

Fig.8. Variations of the power confinements of the fundamental quasi-TM (H_{11}^x) mode with the pitch $\Lambda_0 = 0.35$ mm.

Next, the total power confinement in the air is shown in Fig. 8. Although variation of $\Gamma_{\text{air-core}}$ shows higher peak for higher d_0/Λ_0 value, however, the total power confinement in all the air-holes, $\Gamma_{\text{air-total}}$ shown by pink broken line with down triangles for $d_0/\Lambda_0 = 0.97$ and by a blue solid line with up triangles for $d_0/\Lambda_0 = 0.95$ are almost indistinguishable. However, the pink line reaches a higher maximum confinement factor as its cutoff appears at a higher d_i/Λ_i value. This is because, for a given $\Lambda_0 = 0.35$ mm, the structure with a larger air-hole to pitch ratio reduces the equivalent refractive index of clad (n_{FSM}) and extends the d_i/Λ_i range for the mode to reach its cutoff. Consequently, if a larger the air-hole to pitch ratio is chosen, then more power in the air-holes (both in core and cladding) can be confined before reaching the cutoff limit.

The power confinement is drastically affected by reducing the outer pitch Λ_0 of the PCF. Figure 9 shows the variations of the power confinement for $d_0/\Lambda_0 = 0.97$ but with different Λ_0. By reducing the pitch Λ_0, a PCF can be operated closer to the cutoff condition. For a higher pitch of $\Lambda_0 = 0.35$ mm, the result shows a well-confined of fundamental quasi-TM (H_{11}^x) mode inside the core and reaching a maximum value of the power confinement of air-core. Since, the pitch is larger than the wavelength, the mode is well confined. It should be noted that, as the outer pitch Λ_0 is reduced, the inner pitch Λ_i should also be reduced to maintain their constant ratio of 9, required for this design, with $N_{\text{core}} = 4$. The core size is therefore reduced as the reduction of the outer pitch is considered. Variations of the air-core confinement, $\Gamma_{\text{air-core}}$ and total air-core confinement, $\Gamma_{\text{air-total}}$ are shown in Fig. 10. It should be noted that, we should not operate a PCF very close to its modal cutoff points, but much safer would be to operate this when the $\Gamma_{\text{air-core}}$ shows its maximum value, indicating that mode is well confined inside the core. This identifies a possible optimum design with $\Lambda_0 = 0.35$ mm, $d_0/\Lambda_0 = 0.97$, and $d_i/\Lambda_i = 0.82$, with more than 80% of the power confined in the air-holes. This would reduce the modal loss of Teflon porous core PCF to 26 dB/m from its bulk material loss value of 130 dB/m. However, instead of using identical air-holes in the cladding, by using a higher d_0/Λ_0 in the outer most ring, it is possible to increase confinement in air-holes more than 85% by operating a PCF closer to its modal cutoff without suffering higher leakage and bending losses. This modal loss can be further reduced if we consider a d_0/Λ_0 value larger than 0.97, as taken now and also a larger pitch, Λ. Besides these, if bulk material loss can be further reduced then flexible dielectric waveguides can be designed with a significantly lower modal loss values.

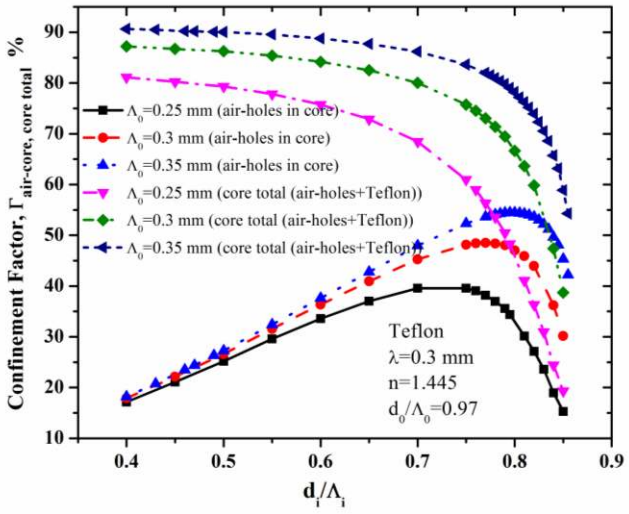

Fig.9. Variations of the power confinements of the fundamental quasi-TM (H_{11}^x) mode with the $d_0/\Lambda_0 = 0.97$

However, besides reducing the modal loss our another aim was to design a low-loss PCF which can also maintain the polarization state. Conventional PCF with hexagonal air-hole arrangement has a 6-fold rotational symmetry. Although, strictly this structure does not have a 90 degrees rotational symmetry but the resultant birefringence is often very small. The modal birefringence of PCF can be increased by breaking the natural symmetry of having identical size air- holes in any given ring. Xxx Earlier, it was shown that, if four out of the six air-holes in the first ring can be different than other two air-holes, then maximum birefringence can be achieved and such structure can also be easily fabricated. Next, the design approach to achieve it would be to increase modal birefringence of the PCF. The resultant asymmetry of the core shape provide an effective index difference between the

H_{11}^x and H_{11}^y modes. It is well known that air-holes in the first ring dominate the modal properties, such as the birefringence of such a PCF. In earlier works [35-37], increasing the air-hole diameters of these four air-holes in the first ring was considered. In reality, as d_2 is either decreased or increased and in both cases as $d_2 \neq d$, the modal index difference between the two fundamental polarized modes will increases.

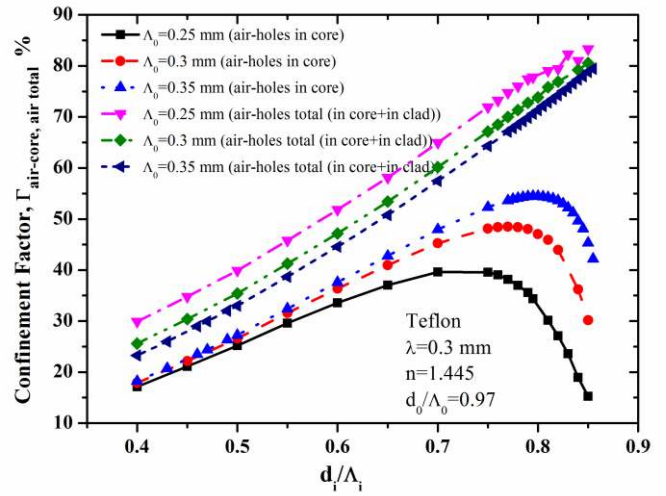

Fig.10. Variations of the power confinements of the fundamental quasi-TM (H_{11}^x) mode with $d_0/\Lambda_0 = 0.97$

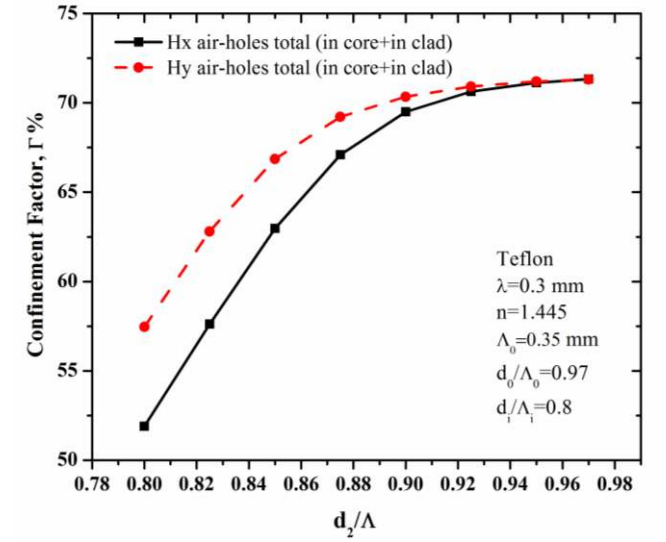

Fig.11. Variation of the power confinement both H_{11}^x and H_{11}^y modes with d_2/Λ

However, here as d_0/Λ_0 for all of cladding air-holes was taken as 0.97, considered to be the maximum value in this study, so in this study, rather than increasing the d_2/Λ_0 value from 0.97, the effect of reduction of air-hole diameter is investigated. The effect of reducing d_2 that is equivalent to changing the four air-holes in the first ring very close to the core are smaller than those of the other air-hole diameters are studied. In Fig. 11, the variation of the power confinements of quasi-TE and quasi-TM modes with the d_2/Λ ratio for $d_i/\Lambda_i = 0.8$ and $\Lambda_0 = 0.35$ mm are shown. It can be observed that the power confinement in air-holes decreases as the value of the diameter d_2 is reduced. This is due to the reduced air-hole diameter, the modal field moves more into the Teflon region so the power confinements in both the core and cladding air-holes decrease.

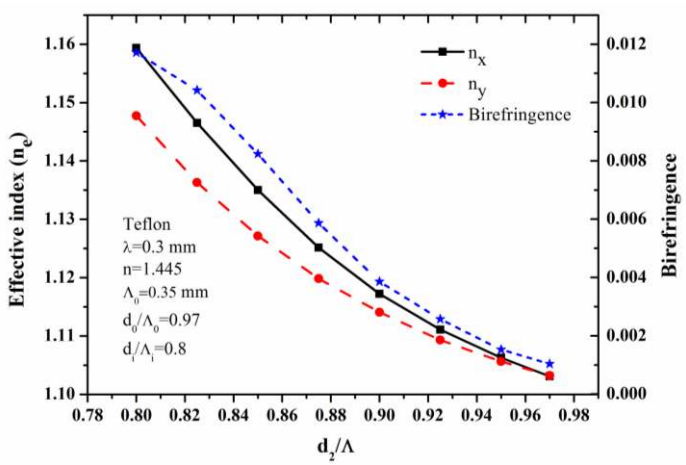

Fig.12. Variation of effective index with d_2/Λ

However, such a PCF would be able to maintain a specific input state of polarization and the corresponding modal birefringence would also be high. Since the influence of the air-holes in the first ring would be dominant to break the structural symmetry in the first ring. For this arrangement as its equivalent height is greater than its equivalent width, $n_e^x > n_e^y$, as a consequence of the effective index of the quasi-TM mode is higher than that of the quasi-TE mode as shown in Fig. 12. It can be clearly observed that as the diameter of d_2 is decreased, effective index increases for both the TE and TM polarizations and the modal index difference between the two fundamental quasi-TE and quasi-TM increases, shown by a blue dotted line with stars. Changing of d_2 makes the PCF structure more asymmetric and it is shown here that birefringence value as large as 0.012 can be easily achieved and this structure can also be easily produced by using simpler stack-and-draw approaches. Although higher birefringence value of 0.026 has been reported earlier [40] but they would require a more complex fabrication process, possibly using the extrusion process.

As d_2 is reduced, the solid cladding area near these air-holes increases and field tends to move there. However, in our earlier work on HiBi PCF, maximum field was always at the center of the core. For the normal PCF, as d_2 increases the cladding area increases, but the center of the whole solid core remains at the center, at $x = 0, y = 0$. But in this case, as the core is not solid, it is rather porous, so its equivalent index is smaller than that of Teflon whereas area in cladding just left d_2 is pure Teflon with a slightly higher index. It can be

observed the field is more confined in the horizontal direction due to the presence of a larger air-hole (with diameter *d*) on the x-axis compared to the field confinement in the vertical direction where a smaller air-hole (with diameter d_2) allows field enhancement there. Field contour showing its maximum location moved up from the center as shown in Fig. 13. When d_2 is reduced further, the mode-field center moves up along the y-axis.

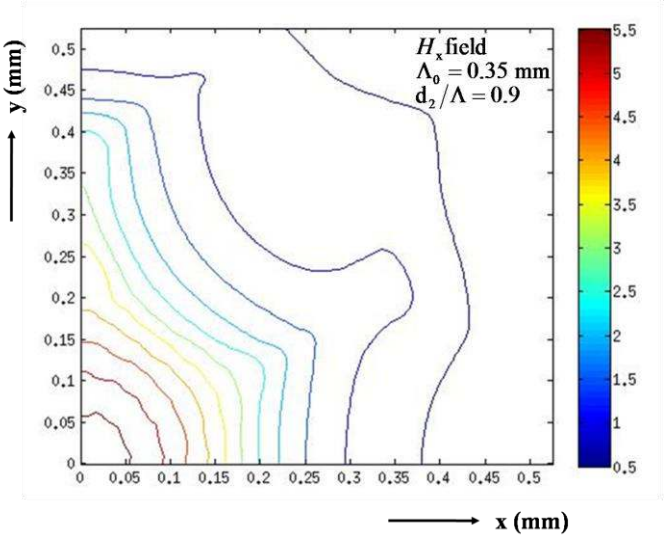

Fig.13. H_x field of the H_{11}^x mode with $d_2/\Lambda = 0.9$, $d_0/\Lambda_0 = 0.97$ and $d_i/\Lambda_i = 0.8$

IV. CONCLUSION

A rigorous finite element approach based on a full-vectorial **H**-field formulation has been used to design and characterize a porous-core Teflon PCF as a THz waveguide. The mode field profile and power confinements, with the variation of waveguide parameters are thoroughly studied to maximize the confinement in the combined air-holes, both in cladding and in cores. It is shown here that more than 85% of the total power can be confined in the air-holes and thus modal loss of such waveguides can also be reduced by 85% of the bulk material loss. With the development of better material and also with the

better control of the fabrication technology, this modal loss value can be reduced further and a viable flexible low-loss dielectric THz waveguide can be obtained. The effect of having unequal size air-holes in the first ring of the cladding to enhance the modal birefringence of such low-loss THz dielectric waveguides is also demonstrated, and such a waveguide can be used where polarization maintenance would be necessary.

REFERENCES

[1] K. Kawase, Y. Ogawa, Y. Watanabe, and H. Inoue, "Non-destructive terahertz imaging of illicit drugs using spectral fingerprints," *Optics Express,* vol. 11, pp. 2549-2554, 2003.

[2] M. W. Ruth, E. C. Bryan, P. W. Vincent, J. P. Richard, D. A. Donald, H. L. Edmund, and P. Michael, "Terahertz pulse imaging in reflection geometry of human skin cancer and skin tissue," *Physics in Medicine and Biology,* vol. 47, p. 3853, 2002.

[3] R. Woodward, V. Wallace, D. Arnone, E. Linfield, and M. Pepper, "Terahertz pulsed imaging of skin cancer in the time and frequency domain," *Journal of Biological Physics,* vol. 29, pp. 257-259, 2003.

[4] M. Pengcheng and X. Long, "The new diagnosing method basing on the frequency analysis of human's nails in T-RAY," *Journal of Physics: Conference Series,* vol. 276, p. 012219, 2011.

[5] A. Y. Pawar, D. D. Sonawane, K. B. Erande, and D. V. Derle, "Terahertz technology and its applications," *Drug Invention Today,* vol. 5, pp. 157-163, 2013.

[6] K. Humphreys, J. P. Loughran, M. Gradziel, W. Lanigan, T. Ward, J. A. Murphy, and C. O'Sullivan, "Medical applications of terahertz imaging: a review of current technology and potential applications in biomedical engineering," in *Engineering in Medicine and Biology Society, 2004. IEMBS '04. 26th Annual International Conference of the IEEE*, pp. 1302-1305, 2004.

[7] D. A. Crawley, C. Longbottom, B. E. Cole, C. M. Ciesla, D. Arnone, V. P. Wallace, and M. Pepper, "Terahertz Pulse Imaging: A Pilot Study of Potential Applications in Dentistry," *Caries Research,* vol. 37, pp. 352-359, 2003.

[8] M. J. Fitch and R. Osiander, "Terahertz waves for communications and sensing," *Johns Hopkins APL technical digest,* vol. 25, pp. 348-355, 2004.

[9] R. H. Jacobsen, D. M. Mittleman, and M. C. Nuss, "Chemical recognition of gases and gas mixtures with terahertz waves," *Optics Letters,* vol. 21, pp. 2011-2013, 1996.

[10] K. Radhanpura, S. Hargreaves, and R. A. Lewis, "The generation of terahertz frequency radiation by optical rectification," *Condensed Matter and Materials Meeting,* pp. 1-4, Wagga Wagga, Australia, 2009.

[11] A. G. Davies, E. H. Linfield, and M. B. Johnston, "The development of terahertz sources and their applications," *Physics in Medicine and Biology,* vol. 47, p. 3679, 2002.

[12] A. E. Fatimy, S. B. Tombet, F. Teppe, W. Knap, D. B. Veksler, S. Rumyantsev, M. S. Shur, N. Pala, R. Gaska, Q. Fareed, X. Hu, D. Seliuta, G. Valusis, C. Gaquiere, D. Theron, and A. Cappy, "Terahertz detection by GaN/AlGaN transistors," *Electronics Letters,* vol. 42, pp. 1342-1343, 2006.

[13] K. Wang and D. M. Mittleman, "Metal wires for terahertz wave guiding," *Nature,* vol. 432, pp. 376-379, 2004.

[14] G. Gallot, S. Jamison, R. McGowan, and D. Grischkowsky, "Terahertz waveguides," *JOSA B,* vol. 17, pp. 851-863, 2000.

[15] J.-T. Lu, Y.-C. Hsueh, Y.-R. Huang, Y.-J. Hwang, and C.-K. Sun, "Bending loss of terahertz pipe waveguides," *Optics Express,* vol. 18, pp. 26332-26338, 2010.

[16] C. Themistos, B. M. A. Rahman, M. Rajarajan, K. T. V. Grattan, B. Bowden, and J. Harrington, "Characterization of silver/polystyrene (PS)-coated hollow glass waveguides at THz frequency," *Journal of Lightwave Technology,* vol. 25, pp. 2456-2462, 2007.

[17] S. Atakaramians, S. Afshar V, T. M. Monro, and D. Abbott, "Terahertz dielectric waveguides," *Advances in Optics and Photonics,* vol. 5, pp. 169-215, 2013.

[18] G. Zhao, M. Ter Mors, T. Wenckebach, and P. C. Planken, "Terahertz dielectric properties of polystyrene foam," *JOSA B,* vol. 19, pp. 1476-1479, 2002.

[19] A. Dupuis, J.-F. Allard, D. Morris, K. Stoeffler, C. Dubois, and M. Skorobogatiy, "Fabrication and THz loss measurements of porous subwavelength fibers using a directional coupler method," *Optics Express,* vol. 17, pp. 8012-8028, 2009.

[20] L.-J. Chen, H.-W. Chen, T.-F. Kao, J.-Y. Lu, and C.-K. Sun, "Low-loss subwavelength plastic fiber for terahertz waveguiding," *Optics Letters,* vol. 31, pp. 308-310, 2006.

[21] H. Han, H. Park, M. Cho, and J. Kim, "Terahertz pulse propagation in a plastic photonic crystal fiber," *Applied Physics Letters,* vol. 80, pp. 2634-2636, 2002.

[22] C. S. Ponseca Jr, R. Pobre, E. Estacio, N. Sarukura, A. Argyros, M. C. Large, and M. A. van Eijkelenborg, "Transmission of terahertz radiation using a microstructured polymer optical fiber," *Optics Letters,* vol. 33, pp. 902-904, 2008.

[23] S. Atakaramians, S. Afshar V, H. Ebendorff-Heidepriem, M. Nagel, B. M. Fischer, D. Abbott, and T. M. Monro, "THz porous fibers: design, fabrication and experimental characterization," *Optics Express,* vol. 17, pp. 14053-14062, 2009.

[24] K. Nielsen, H. K. Rasmussen, A. l. J. L. Adam, P. C. M. Planken, O. Bang, and P. U. Jepsen, "Bendable, low-loss Topas fibers for the terahertz frequency range," *Optics Express,* vol. 17, pp. 8592-8601, 2009.

[25] M. Goto, A. Quema, H. Takahashi, S. Ono, and N. Sarukura, "Teflon photonic crystal fiber as terahertz waveguide," *Japanese Journal of Applied Physics,* vol. 43, p. L317, 2004.

[26] M. Goto, A. Quema, H. Takahashi, S. Ono, and N. Sarukura, "Teflon photonic crystal fiber as polarization-preserving waveguide in THz region," *Ultrafast Phenomena XIV: Proceedings of the 14th International Conference, Niigata, Japan, July 25â€“30, 2004,* pp. 702-704, 2005.

[27] M. Skorobogatiy and A. Dupuis, "Ferroelectric all-polymer hollow Bragg fibers for terahertz guidance," *Applied Physics Letters,* vol. 90, p. 113514, 2007.

[28] J.-Y. Lu, C.-P. Yu, H.-C. Chang, H.-W. Chen, Y.-T. Li, C.-L. Pan, and C.-K. Sun, "Terahertz air-core microstructure fiber," *Applied Physics Letters,* vol. 92, p. 064105, 2008.

[29] B. Ung, A. Mazhorova, A. Dupuis, M. Roze, and M. Skorobogatiy, "Polymer microstructured optical fibers for terahertz wave guiding," *Optics Express,* vol. 19, pp. B848-B861, 2011.

[30] H. Bao, K. Nielsen, H. K. Rasmussen, P. U. Jepsen, and O. Bang, "Fabrication and characterization of porous-core honeycomb bandgap THz fibers," *Optics Express,* vol. 20, pp. 29507-29517, 2012.

[31] K. Nielsen, H. K. Rasmussen, P. U. Jepsen, and O. Bang, "Porous-core honeycomb bandgap THz fiber," *Optics Letters,* vol. 36, pp. 666-668, 2011.

[32] S. Atakaramians, S. A. V, B. M. Fischer, D. Abbott, and T. M. Monro, "Porous fibers: a novel approach to low loss THz waveguides," *Optics Express,* vol. 16, pp. 8845-8854, 2008.

[33] M. Uthman, B. M. A. Rahman, N. Kejalakshmy, A. Agrawal, and K. T. V. Grattan, "Design and Characterization of Low-Loss Porous-Core Photonic Crystal Fiber," *Photonics Journal, IEEE,* vol. 4, pp. 2315-2325, 2012.

[34] A. Hassani, A. Dupuis, and M. Skorobogatiy, "Porous polymer fibers for low-loss Terahertz guiding," *Optics Express,* vol. 16, pp. 6340-6351, 2008.

[35] N. Kejalakshmy, B. M. A. Rahman, A. Agrawal, T. Wongcharoen, and K. Grattan, "Characterization of single-polarization single-mode photonic crystal fiber using full-vectorial finite element method," *Applied Physics B,* vol. 93, pp. 223-230, 2008.

[36] B. M. A. Rahman, M. Uthman, N. Kejalakshmy, A. Agrawal, and K. T. V. Grattan, "Design of bent photonic crystal fiber supporting a single polarization," *Applied Optics,* vol. 50, pp. 6505-6511, 2011.

[37] B. M. A. Rahman, A. Kabir, M. Rajarajan, K. T. V. Grattan, and V. Rakocevic, "Birefringence study of photonic crystal fibers by using the full-vectorial finite element method," *Applied Physics B,* vol. 84, pp. 75-82, 2006.

[38] T. P. Hansen, J. Broeng, S. E. Libori, E. Knudsen, A. Bjarklev, J. R. Jensen, and H. Simonsen, "Highly birefringent index-guiding photonic crystal fibers," *Photonics Technology Letters, IEEE,* vol. 13, pp. 588-590, 2001.

[39] B. M. A. Rahman and J. B. Davies, "Finite-element analysis of optical and microwave waveguide problems," *Microwave Theory and Techniques, IEEE Transactions on,* vol. 32, pp. 20-28, 1984.

[40] S. Atakaramians, S. Afshar V, B. M. Fischer, D. Abbott, and T. M. Monro, "Low loss, low dispersion and highly birefringent terahertz porous fibers," *Optics Communications,* vol. 282, pp. 36-38, 2009.

Asmar Aming received B.Sc. degree in physics from Kasetsart University, Thailand, in 2008 and M.Sc. in 2011 from Mahidol University. She is now Ph.D. student in Mahidol University, Thailand.

In 2015, she joined photonic research group, City University London, London, U.K. as research assistant. Her research interest includes numerical modeling of photonic crystal fiber in optical and Terahertz region using finite element method.

Muhammad Uthman received B.Eng. in Electrical Engineering, in 2004 from Ahmadu Bello University, Zaria, Nigeria and M.Sc. in Telecommunications and Networks with

Distinction, in 2008 from City University, London. He also received Ph.D. degree in Electrical Engineering from City University London, London, U.K. in 2013. His research interests include numerical modeling and simulation microstructure optical fiber and waveguide at optical and THz frequencies and the application of finite-element method-based approaches for the characterization of photonic devices.

Ratchapak Chitaree received the B.Sc. in Physics from Mahidol University in 1990 and his Ph.D. degree from City University London, London, U.K. in 1994. His research interests include design and fabrication long period fiber grating in optical range, Generation and investigation of the rotating polarized light by various types of interferometer and numerical modeling optical and Terahertz waveguide.

Waleed Mohammed received B.Sc. from the department of electronics and electrical communications, Faculty of Engineering, in 1996 with a major in control systems and M.Sc. degree from the department of computer engineering, Cairo University, Giza, Egypt in 1999. In the same year he joined the College of optics and photonics/CREOL, University of Central Florida, Orlando, FL, USA as a research assistant and he received M.Sc. degree in optics in 2001. He completed his Ph.D. work in 2004 and his thesis was titled “nano/micro optical elements for mode coupling applications. He joined ultra-fast photonics laboratory (UPL), Electrical and Computer Engineering department, University of Toronto, as a postdoctoral fellow in 2004-2007. In 2007, Dr. Mohammed joined the International School of Engineering, Chulalongkorn University as a lecturer in the nano-engineering program. In 2010 Dr. Mohammed joined the School of Engineering, Bangkok University where is currently a research scholar.

B. M. Azizur Rahman (S’80–M’83–SM’94-F’2016) received the B.Sc.Eng and M.Sc.Eng. degrees in electrical engineering with distinctions from Bangladesh University of Engineering and Technology (BUET), Dhaka, Bangladesh, in 1976 and 1979, respectively. He also received two gold medals for being the best undergraduate and graduate students of the university in 1976 and 1979, respectively. In 1979, he was awarded with a Commonwealth Scholarship to study for a Ph.D. degree in the U.K. and subsequently in 1982 received the Ph.D. degree in electronics from University College London,U.K.

From 1976 to 1979, he was a Lecturer at the Electrical Engineering Department, BUET. In 1982, after receiving the PhD degree, he joined University College London as a Postdoctoral Research Fellow and continued his research work on the development of finite element method for characterising optical guided-wave devices. In 1988, he joined City University of London, as a Lecturer, where he is now a Professor. At City University, he leads the research group on Photonics Modelling, specialised in the use of rigorous and full-vectorial numerical approaches to design, analyse and optimise a wide range of photonic devices, such as spot-size converters, high-speed optical modulators, compact bend designs, power splitters, polarisation splitters, polarisation rotators, polarization controllers, terahertz devices, etc. He has published more than 500 journal and conference papers, and his journal papers have been cited more than 3400 times. Prof. Rahman is a Fellow of the IEEE, the Optical Society of America, and the International Society for Optical Engineering (SPIE).